

**Proceedings of the INMM & ESARDA Joint Virtual Annual Meeting  
August 23-26 & August 30-September 1, 2021**

Application of  $\gamma$ - $\gamma$  Coincidence Technique with CLLBC Detectors to Enhance  $^{134}\text{Cs}$  Gamma Signal  
in a Mixed Gamma Field

**J. Joshi, W. Charlton**

The University of Texas, Austin, Texas, USA

E-mail : [jay.joshi@utexas.edu](mailto:jay.joshi@utexas.edu), [wcharlton@austin.utexas.edu](mailto:wcharlton@austin.utexas.edu)

**ABSTRACT:**

Measurement and quantification of fission products such as  $^{134}\text{Cs}$ ,  $^{137}\text{Cs}$ , and  $^{154}\text{Eu}$  can be used to determine the burnup of used nuclear fuel by measuring the intensity of the gamma signals emitted via gamma-ray spectrometry. However, used nuclear fuel is comprised of several other fission products that produce a large gamma background, which makes it hard to accurately isolate gamma signals of interest (605 keV line from  $^{134}\text{Cs}$ ) from the background signal from these other fission products (especially the 661 keV line from  $^{137}\text{Cs}$ ). One of the techniques that could solve this issue is by applying the  $\gamma$ - $\gamma$  coincidence technique to remove uncorrelated gamma-ray noise from the time-correlated gamma signals from  $^{134}\text{Cs}$ . In this study, two CLLBC scintillation detectors with good resolution ( $\sim 3.5\%$  at 662 keV) were used to acquire LIST mode gamma-ray spectra from a complex gamma source containing  $^{134}\text{Cs}$ ,  $^{137}\text{Cs}$ ,  $^{60}\text{Co}$ , and  $^{154}\text{Eu}$ . CLLBC detectors have reasonably good energy resolution, are portable (potentially useable in an underwater safeguards instrument), and have the ability to simultaneously measure neutron counts using pulse shape discrimination. The LIST mode data acquired was processed with a  $\gamma$ - $\gamma$  coincidence algorithm to eliminate the uncorrelated background counts. The signal-to-background ratio in the prominent gamma peaks of the fission product isotope  $^{134}\text{Cs}$  are compared between singles and coincidence spectra. This work demonstrated the concept of using  $\gamma$ - $\gamma$  coincidence counting to quantitatively measure the  $^{134}\text{Cs}$  content in a mixed gamma source using CLLBC detectors.

**Introduction**

One of the International Atomic Energy Agency (IAEA) missions is to verify states' compliance with their safeguards agreements preventing the diversion of safeguarded nuclear material to a clandestine weapons program[1]. To accomplish this, nuclear material (NM) diversion must be detected in a timely manner. The IAEA must verify the correctness and completeness of the State's declaration. Nuclear material accountancy is the IAEA's primary verification method in which the IAEA's safeguards inspectors perform impartial measurements to verify the amount of NM declared by the State's accounts. Non-destructive analysis (NDA) techniques are often used by the IAEA safeguards inspectorates to verify the operator's records. NDA techniques may include procedures such as: physically counting NM containers or fuel rods/assemblies, weighing items, or measuring radiation emitted by an item (e.g., Cherenkov radiation, neutrons, or gamma rays)[1].

Research reactor used fuel safeguards verification may include verifying fuel parameters such as initial enrichment, burnup, cooling time, and residual fissile mass ( $^{235}\text{U} + ^{239}\text{Pu}$ ). Various safeguards instruments that rely on neutron and gamma signal measurements may be used to quantify such fuel parameters.  $^{134}\text{Cs}$ ,  $^{137}\text{Cs}$ , and  $^{154}\text{Eu}$  are prominent fission product gamma-ray sources in used nuclear fuel, and their activity is proportional to the fuel burnup and inversely proportional to the cooling time. Researchers have performed gamma spectrometry of used fuel in the past to obtain the

$^{134}\text{Cs}/^{137}\text{Cs}$  and  $^{154}\text{Eu}/^{137}\text{Cs}$  gamma activity to determine burnup and cooling time of commercial used fuel for international safeguards verification[2-3].

While the isotopic content of used nuclear fuel (e.g.,  $^{137}\text{Cs}$ ,  $^{134}\text{Cs}$ , and  $^{154}\text{Eu}$ ) may be obtained through gamma spectroscopy, their content increases with burnup and decreases with cooling time. Quantification of  $^{134}\text{Cs}$  for burnup verification can be complex. For example, when the cooling time of used fuel is very short (<2 years), the activity of  $^{134}\text{Cs}$  is very high; however, when cooling time is longer (>5 years), the  $^{137}\text{Cs}$  activity dominates the spectrum[2]. The gamma lines from  $^{134}\text{Cs}$  can be indistinguishable due to the high Compton background from  $^{137}\text{Cs}$  and other isotopes. While  $^{137}\text{Cs}$  produces a single gamma line at 661 keV,  $^{134}\text{Cs}$  produces multiple time-correlated gamma lines. Therefore, removing gamma lines that are not time correlated can eliminate the background from time-correlated gamma lines. Multiple gamma spectroscopy detectors would be used in such detection systems, with all detectors time-synchronized and the energy calibrated. A gamma-ray pulse would be recorded only if the detection system detects another gamma-ray pulse inside the defined time interval (a coincidence gate). The data collection system would reject many of the uncorrelated gamma rays.

There are two methods to set up a coincidence gate for  $\gamma$ - $\gamma$  coincidence counting:

1. In the case of a mixed gamma source with unknown composition, every pair of pulses are recorded that occur within a specified coincidence time window. Any pulses that occur outside that time window are ignored. This will eliminate most of the uncorrelated gamma rays and allow for identification of all unknown radioactive isotopes that emit correlated gamma rays. This is the method used in this study.
2. In the second case, the coincidence time gate is applied to a specific gamma peak. In this case if there is an expectation of the isotopic content of the sample, then the gated system will record all pulses within the coincidence time gate when a pulse within the peak of interest is recorded. This eliminates additional background and nuisance signals from the recorded events. There will be  $^{134}\text{Cs}$ ,  $^{137}\text{Cs}$ , and  $^{154}\text{Eu}$  in the nuclear reactor used fuel. Therefore, instead of setting up a coincidence gate for everything, the coincidence gate could be applied to a specific gamma line. For example, a coincidence gate could be applied to the 604 keV gamma line of  $^{134}\text{Cs}$ . With this, anything that is not in coincidence with the 604 keV gamma line will be eliminated. This could then be repeated for any gamma line of interest. This method may have advantages for nuclear reactor used fuel safeguards. Therefore, future work will be performed utilizing the later approach[4].

Table 1 shows a list of  $^{134}\text{Cs}$  gamma lines with their corresponding intensities and coincident gamma lines. We can see that the major correlated gamma lines of  $^{134}\text{Cs}$  are 569.33 keV, 604.72 keV, 795.86 keV, and 801.95 keV. However, detectors used in this study cannot fully resolve the 569.33 keV gamma line from 604 keV and 801.86 keV from 795.86 keV gamma lines. Since the former two and later two gamma lines are also time-correlated, they do not need to be differentiated. They can be regarded as one gamma line for peak analysis and their branching ratios adjusted accordingly[2, 5-6].

**Table 1:  $^{134}\text{Cs}$  gamma lines, relative intensities, and corresponding coincident gamma lines [2]**

| <b>E(keV)</b> | <b><math>I_{\gamma}</math>(%)</b> | <b>Coincident Gamma lines (keV)</b>                             |
|---------------|-----------------------------------|---|
| <b>232.6</b>  | 0.001                             | 242.74, 326.59, 563.25, 569.33, 604.72, 1167.97                 |
| <b>242.74</b> | 0.027                             | 232.6, 326.59, 563.25, 604.72, 795.86, 1167.97                  |
| <b>326.59</b> | 0.016                             | 232.6, 242.74, 475.36, 563.25, 604.72, 795.86, 1038.61, 1167.97 |

|                |       |  |
|----------------|-------|--|
| <b>475.36</b>  | 1.479 | 326.59, 563.25, 604.72, 1167.97  |
| <b>563.25</b>  | 8.342 | 232.6, 242.74, 326.59, 475.36, 569.33, 604.72, 801.95                      |
| <b>569.33</b>  | 15.37 | 232.6, 563.25, 604.72, 795.86, 1167.97                                     |
| <b>604.72</b>  | 97.63 | 232.6, 242.7, 326.6, 475.36, 563.25, 569.3, 795.86, 801.95, 1038.6, 1365.2 |
| <b>795.86</b>  | 85.47 | 242.74, 326.59, 569.33, 604.72   |
| <b>801.95</b>  | 8.694 | 563.25, 604.72, 1167.97  |
| <b>1038.61</b> | 0.99  | 326.59, 604.72   |
| <b>1167.97</b> | 1.791 | 232.6, 242.74, 326.59, 475.36, 569.33, 801.95                              |
| <b>1365.18</b> | 3.019 | 604.72   |

In this paper, we focus on examining the feasibility of  $\gamma$ - $\gamma$  coincidence measurements with  $\text{Cs}_2\text{LiLa}(\text{Br},\text{Cl})_6:\text{Ce}$  (CLLBC) detectors with approximately 3.5% energy resolution at 661 keV for safeguards on research reactor used fuel. CLLBC scintillation detectors can simultaneously measure neutrons and gamma rays using pulse shape discrimination. This capability might allow simultaneous  $\gamma$ - $\gamma$  coincidence and neutron coincidence measurements for used fuel safeguards verification. Unlike traditional high-resolution high-purity germanium (HPGe) detectors, CLLBC scintillator detectors don't need cooling[7-8]. They are portable and can handle relatively high gamma count rates, making them appropriate for the underwater measurement of used fuel[9-10].

### Instrument setup

Four CLLBC gamma/neutron scintillation detectors were set up in a coincidence layout as shown in Figure 1. This setup used the Xia Pixie-16  $\gamma$ - $\gamma$  coincidence system in LIST mode to analyze the signals from the measurement system. Four detectors were used to increase the overall  $\gamma$ - $\gamma$  coincidence efficiency. Lead shielding was placed above, below, and around the detectors to attenuate the  $^{40}\text{K}$  high-energy gamma-ray background at 1460 keV and to limit the likelihood of gamma-rays scattering in one detector and then interacting in a second detector. The radiation sources were placed at the center of the detectors. Two source configurations were used: (1) a mixture of  $^{137}\text{Cs}$  and  $^{134}\text{Cs}$  sources in which the  $^{137}\text{Cs}$  intensity is higher than the  $^{134}\text{Cs}$  intensity and (2) a mixture of  $^{134}\text{Cs}$ ,  $^{154}\text{Eu}$ ,  $^{137}\text{Cs}$ , and  $^{60}\text{Co}$  sources in which the  $^{137}\text{Cs}$  intensity was varied. Figure 1(a) shows  $\gamma$ - $\gamma$  coincidence measurement setup with four CLLBC detectors and gamma sources at the center, and Figure 1(b) shows the final setup with lead shielding around the detectors.

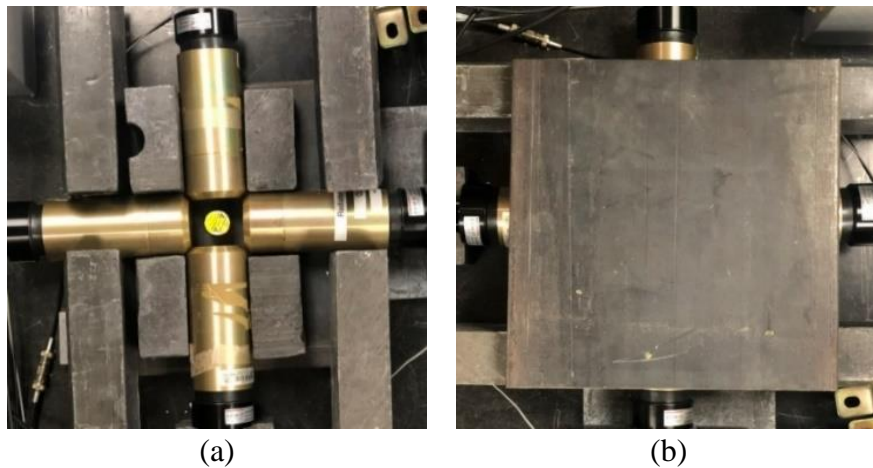


**Figure 1: (a) CLLBC  $\gamma$ - $\gamma$  coincidence setup with four detectors with gamma sources at the center and (b)  $\gamma$ - $\gamma$  coincidence setup with shielding over detectors.**

## Results and Analysis

To check the feasibility of the  $\gamma$ - $\gamma$  coincidence technique with CLLBC detectors, a simple gamma source with  $^{134}\text{Cs}$  and  $^{137}\text{Cs}$  was measured using two CLLBC detectors in the coincidence setup. Figure 2 shows a normal and  $\gamma$ - $\gamma$  coincidence spectra of a combined  $^{134}\text{Cs}$  and  $^{137}\text{Cs}$  fixed gamma source acquired using PeakEasy. The spectra show that the uncorrelated 661 keV gamma-rays from  $^{137}\text{Cs}$  are almost eliminated when a coincidence gate is applied to the  $\gamma$ - $\gamma$  list mode data.

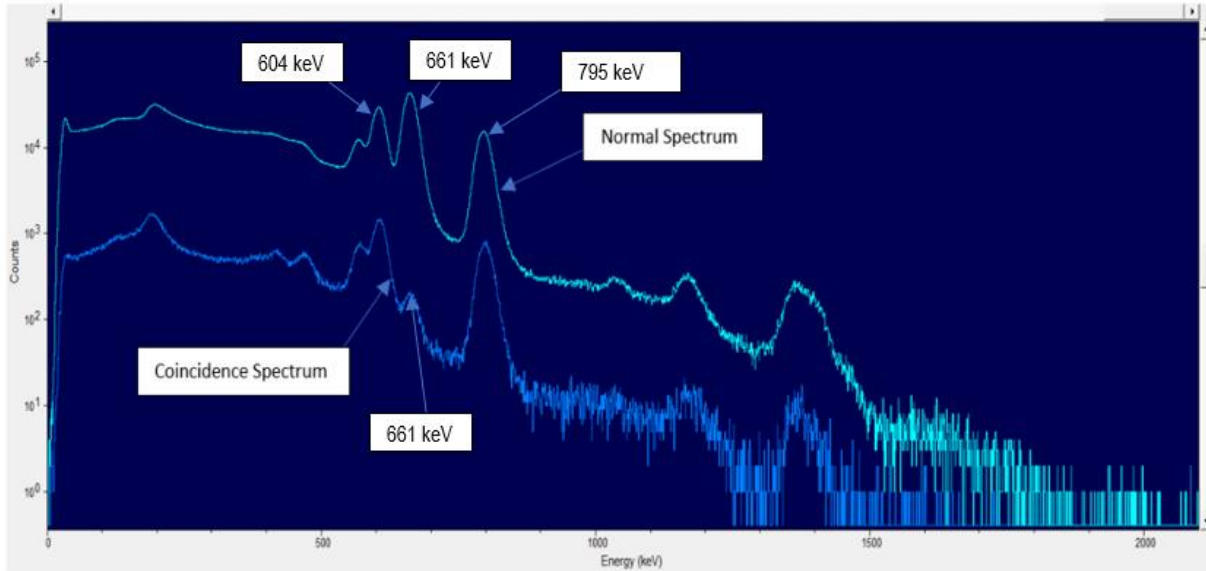


**Figure 2: Normal and background suppressed  $\gamma$ - $\gamma$  coincidence spectra of  $^{134}\text{Cs}$  and  $^{137}\text{Cs}$  fixed gamma source acquired from PeakEasy**

To quantify the improvement shown in Figure 2, the signal-to-noise ratio in the  $^{134}\text{Cs}$  prominent gamma peaks (604 keV and 795 keV) was calculated and compared between the normal and coincident spectra. The signal-to-noise (S/N) ratio was calculated by dividing net counts in the peak by the total counts in the Compton continuum. Table 2 shows the S/N for the normal mode spectrum [denoted (S/N)<sub>n</sub>], the S/N ratio for the coincident mode spectrum [denoted (S/N)<sub>c</sub>], and the ratio of signal-to-noise ratios in coincidence spectrum to the normal spectrum (denoted C/N) under the 604 keV and 795 keV gamma peaks. The results show that the  $\gamma$ - $\gamma$  coincidence measurements increased the signal-to-noise ratio in the 604 keV and 795 keV peaks by approximately 35% for each peak.

**Table 2: S/N ratios in normal and coincidence spectrum and C/N ratios**

| Energy (keV) | (S/N) <sub>n</sub> | (S/N) <sub>c</sub> | C/N           |
|--------------|--------------------|--------------------|---------------|
| <b>604</b>   | 0.044±8.64E-05     | 0.059±5.26E-04     | 1.33±1.21E-02 |
| <b>795</b>   | 0.038±5.82E-05     | 0.053±3.52E-04     | 1.38±9.40E-03 |

A spectrum was taken with the four CLLBC detectors and with four radiation sources combined:  $^{134}\text{Cs}$ ,  $^{137}\text{Cs}$ ,  $^{60}\text{Co}$ , and  $^{154}\text{Eu}$ . These four isotopes are the most prominent fission and activation product gamma-ray sources in used nuclear fuel. The activity of these fission products is proportional to the fuel burnup and inversely proportional to the cooling time. Multiple measurements were performed with the activity of the  $^{134}\text{Cs}$ ,  $^{60}\text{Co}$ , and  $^{154}\text{Eu}$  fixed while the activity of the  $^{137}\text{Cs}$  was varied from 1 to 13  $\mu\text{Ci}$ . The activity of  $^{134}\text{Cs}$ ,  $^{154}\text{Eu}$ , and  $^{60}\text{Co}$  used in this experiment was 3.97  $\mu\text{Ci}$ , 7.77  $\mu\text{Ci}$ , and 2  $\mu\text{Ci}$ , respectively. Figure 3 shows normal spectra, and Figure 4 shows coincidence

spectra with varying  $^{137}\text{Cs}$  activity. Figure 3 shows the varying peak intensity at 661 keV (proportional of course to the activity of the source) as well as prominent  $^{134}\text{Cs}$  peaks at 604 keV and 795 keV. It can be seen that as the intensity of the  $^{137}\text{Cs}$  peak increases, the peak begins to impact the ability to resolve the 604 keV peak from  $^{134}\text{Cs}$ . Figure 4 shows the spectra with a suppressed  $^{137}\text{Cs}$  photopeak at 661 keV which has little to no impact on the 604 keV line.

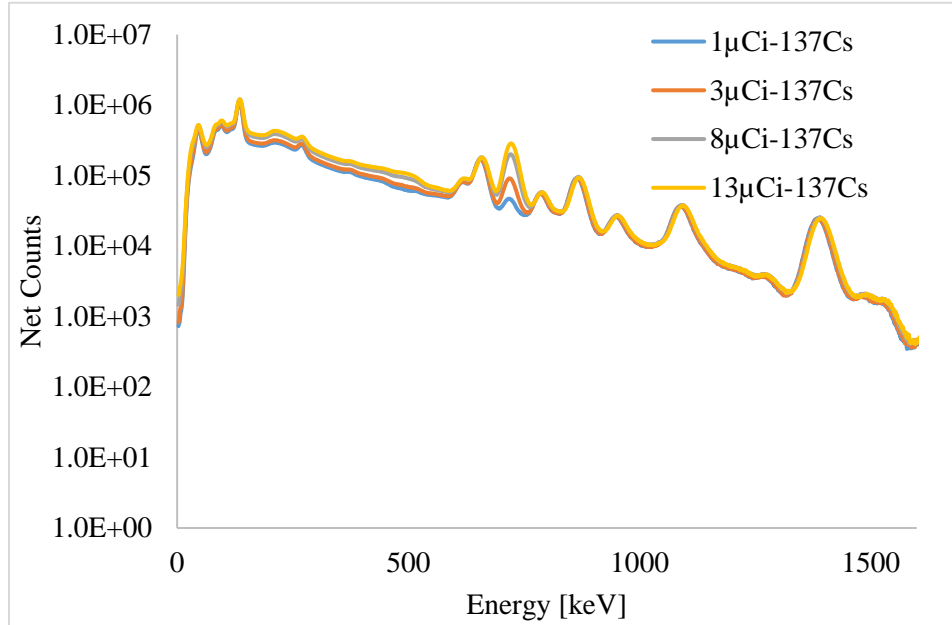


**Figure 3: Normal spectra of combined  $^{134}\text{Cs}$ ,  $^{154}\text{Eu}$ ,  $^{60}\text{Co}$ , and  $^{137}\text{Cs}$  gamma source**

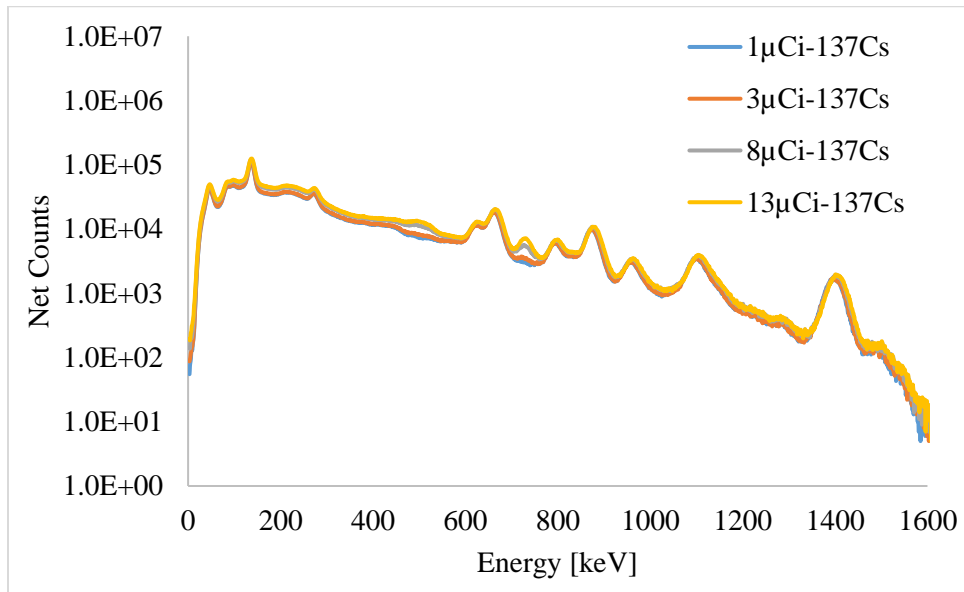


**Figure 4:  $\gamma$ - $\gamma$  coincidence spectra of combined  $^{134}\text{Cs}$ ,  $^{154}\text{Eu}$ ,  $^{60}\text{Co}$ , and  $^{137}\text{Cs}$  gamma source**

The spectra from Figures 3 and 4 were analyzed and the signal-to-noise ratios for the 604 keV and 795 keV gamma-rays of  $^{134}\text{Cs}$  for the normal and  $\gamma$ - $\gamma$  coincidence spectra are shown in Tables 3 and 4. The S/N in the normal spectrum for the 604 keV peak is almost twice that of the 795 keV peak which is mainly due to the higher intensity of the 604 keV line. However, in the coincidence

spectrum, the S/N ratio for the 604 keV line is almost three times that for the 795 keV peak. Also, the S/N ratio for the coincidence spectra for both the 604 and 795 keV lines only vary slightly with the increase in the  $^{137}\text{Cs}$  activity.

**Table 3: S/N ratios in normal spectra**

| $^{137}\text{Cs}$ Activity<br>[ $\mu\text{Ci}$ ] | [S/N] <sub>604 keV</sub> | Standard Deviation<br>[S/N] <sub>604 keV</sub> | [S/N] <sub>795 keV</sub> | Standard Deviation<br>[S/N] <sub>795 keV</sub> |
|--|--------------------------|--|--------------------------|--|
| 1  | 3.64E-02                 | 8.06E-05                                       | 1.63E-02                 | 3.68E-05                                       |
| 3  | 3.19E-02                 | 6.20E-05                                       | 1.51E-02                 | 4.25E-05                                       |
| 8  | 2.52E-02                 | 7.76E-05                                       | 1.24E-02                 | 2.70E-05                                       |
| 13   | 2.23E-02                 | 6.21E-05                                       | 1.17E-02                 | 2.64E-05                                       |

**Table 4: S/N ratios in  $\gamma$ - $\gamma$  coincidence spectra**

| $^{137}\text{Cs}$ Activity<br>[ $\mu\text{Ci}$ ] | [S/N] <sub>604 keV</sub> | Standard Deviation<br>[S/N] <sub>604 keV</sub> | [S/N] <sub>795 keV</sub> | Standard Deviation<br>[S/N] <sub>795 keV</sub> |
|--|--------------------------|--|--------------------------|--|
| 1  | 4.05E-02                 | 2.57E-04                                       | 1.41E-02                 | 1.08E-04                                       |
| 3  | 3.90E-02                 | 2.28E-04                                       | 1.42E-02                 | 1.30E-04                                       |
| 8  | 3.56E-02                 | 2.06E-04                                       | 1.34E-02                 | 1.20E-04                                       |
| 13   | 3.34E-02                 | 2.08E-04                                       | 1.29E-02                 | 1.05E-04                                       |

Using the data from Tables 3 and 4, the ratio of the coincidence-to-normal spectrum signal-to-noise ratios were calculated. These C/N values for varying  $^{137}\text{Cs}$  activity are shown in Figure 5.

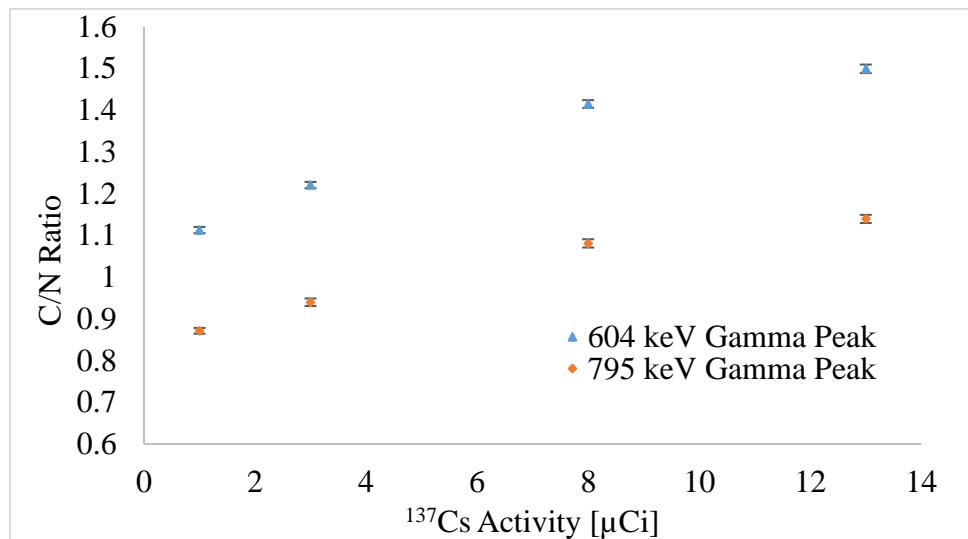


**Figure 5: Ratio of the signal-to-noise ratio in coincidence spectrum to normal spectrum for mixed gamma source with various  $^{137}\text{Cs}$  gamma activity**

Figure 5 shows the effectiveness of the application of the  $\gamma$ - $\gamma$  coincidence technique to the mixed gamma source with various  $^{137}\text{Cs}$  activity strength. In the case of 604 keV gamma peak, the boost in signal-to-noise ratio ranges from 10% for  $1\mu\text{Ci}$  of  $^{137}\text{Cs}$  to approximately 50% for  $13\mu\text{Ci}$  of  $^{137}\text{Cs}$ . However, in the 795 keV gamma peak, the S/N ratio is lower for the 1 and 3 mCi cases compared to the normal spectrum. This is due to the occasional incorrect rejection of a coincidence photon using

this technique. So, a boost in S/N ratio occurs when the  $^{137}\text{Cs}$  activity is higher than  $8\mu\text{Ci}$ . Thus, we see that the  $\gamma\text{-}\gamma$  coincidence technique is most useful when the activity of  $^{137}\text{Cs}$  (and by extension any other nuisance sources) is high.

This complex gamma measurement is roughly analogous to a real-world measurement of nuclear reactor used fuel. The main objective of utilizing  $^{134}\text{Cs}$ ,  $^{137}\text{Cs}$ , and  $^{154}\text{Eu}$  gamma sources was to simulate the primary fission products in used fuel. Figure 5 shows that the use of the  $\gamma\text{-}\gamma$  coincidence technique would be beneficial to quantify prominent  $^{134}\text{Cs}$  gamma rays. When the cooling time of used fuel is long enough such that the  $^{134}\text{Cs}$  lines are no longer visible, the  $^{154}\text{Eu}$  lines would be useable with the same basic technique. Thus, the data acquired here suggests that  $\gamma\text{-}\gamma$  coincidence measurements using CLLBC detectors for complex gamma-emitting sources such as used fuel is feasible. This study also indicates that the  $\gamma\text{-}\gamma$  coincidence technique may help improve the accuracy of the measurement of various other radiation sources in the presence of an intense background or nuisance source. Note that the  $\gamma\text{-}\gamma$  coincidence technique may not be appropriate for commercial LWR fuel assemblies due to their large dimensions and number of pins. The probability of recording coincident gamma lines emitted anywhere in the fuel assembly would be very small due to a large self-shielding and a large fuel assembly dimension. However, it may be useful for measuring individual LWR pins. Research reactor fuel assemblies have smaller dimensions; therefore, this technique may be utilized to enhance burnup indicator quantification.

### **Conclusion and Future Work**

Burnup quantification of used nuclear fuel is difficult in part because of the high gamma background from the fission and activation products and actinides. Accurate quantification of the most prominent fission product burnup indicators such as  $^{134}\text{Cs}$ ,  $^{137}\text{Cs}$ , and  $^{154}\text{Eu}$  is vital to determine the nuclear fuel burnup for nuclear safeguards. Traditionally,  $^{134}\text{Cs}/^{137}\text{Cs}$  and  $^{154}\text{Eu}/^{137}\text{Cs}$  gamma activity ratios are used to verify burnup, but the complexity of these fission products depends on the used fuel cooling time. The half-life of  $^{137}\text{Cs}$  is significantly larger than the half-lives of  $^{134}\text{Cs}$  and  $^{154}\text{Eu}$ , which causes quantification of  $^{134}\text{Cs}$  and  $^{154}\text{Eu}$  complex as cooling time increases. This is because the gamma peak of  $^{137}\text{Cs}$  remains constant over a long time while the  $^{134}\text{Cs}$  and  $^{154}\text{Eu}$  decay away. At some point in time,  $^{137}\text{Cs}$  activity, including its Compton scattered photons, overwhelms  $^{134}\text{Cs}$  and  $^{154}\text{Eu}$  activity. While  $^{137}\text{Cs}$  produce a single uncorrelated gamma-ray at 661 keV,  $^{134}\text{Cs}$  and  $^{154}\text{Eu}$  produce multiple time-correlated gamma-rays during their radioactive decays. Therefore, the  $\gamma\text{-}\gamma$  coincidence technique may help eliminate uncorrelated gamma background due to fission and activation products, especially from  $^{137}\text{Cs}$ , from the fission product indicators [ $^{134}\text{Cs}$  and  $^{154}\text{Eu}$ ], to enhance burnup quantification. In this study, CLLBC scintillation detectors with good resolution ( $\sim 3.5\%$  at 662 keV) were used to acquire LIST mode gamma-ray spectra from a complex gamma source containing  $^{134}\text{Cs}$ ,  $^{137}\text{Cs}$ ,  $^{60}\text{Co}$ , and  $^{154}\text{Eu}$ . The study focused on two main gamma lines of  $^{134}\text{Cs}$  [604 keV and 795 keV]. Multiple measurements were performed with fixed  $^{134}\text{Cs}$ ,  $^{60}\text{Co}$ , and  $^{154}\text{Eu}$ , while variable  $^{137}\text{Cs}$  gamma activity. We obtained a higher S/N ratio in the prominent gamma peaks of  $^{134}\text{Cs}$  when the  $\gamma\text{-}\gamma$  coincidence measurement technique was used. In the case of the 604 keV gamma peak, the boost in signal-to-noise ratio ranged from 10% for  $1\mu\text{Ci}$  of  $^{137}\text{Cs}$  to approximately 50% for  $13\mu\text{Ci}$  of  $^{137}\text{Cs}$ . However, in the 795 keV gamma peak, the boost only appears around  $8\mu\text{Ci}$  and above. For  $1\mu\text{Ci}$  and  $3\mu\text{Ci}$  of  $^{137}\text{Cs}$ , the normal spectra seem to provide a higher signal-to-noise ratio. The reason for this is twofold (1) the contribution of uncorrelated gamma background from 661 keV gamma line of  $^{137}\text{Cs}$  would obviously be significantly higher to its left (lower energy) on the gamma spectrum and (2) the application of coincidence gate for  $\gamma\text{-}\gamma$  coincidence measurement causes significant loss of counts

under the signal as well as Compton continuum. Nonetheless, this work shows the feasibility of the  $\gamma$ - $\gamma$  coincidence technique with CLLBC detectors to enhance  $^{134}\text{Cs}$  Gamma Signal in a Mixed Gamma Field.

### Acknowledgments

This research was performed under the appointment to the Nuclear Nonproliferation International Safeguards Fellowship Program sponsored by the National Nuclear Security Administration's Office of International Nuclear Safeguards (NA-241).

### References

1. IAEA, "Safeguards Techniques and Equipment: 2003 Edition," International Atomic Energy Agency, Austria, August 2003. [https://www-pub.iaea.org/MTCD/Publications/PDF/NVS1-2003\\_web.pdf](https://www-pub.iaea.org/MTCD/Publications/PDF/NVS1-2003_web.pdf).
2. J. Joshi and W. Charlton, "Application of  $\gamma$ - $\gamma$  Coincidence Measurement of  $^{134}\text{Cs}$  and  $^{154}\text{Eu}$  to Verify Burnup and Cooling Time for TRIGA Reactor Used Fuels at the University of Texas Nuclear Engineering Teaching Laboratory," INMM Annual Meeting; Palm Desert, CA USA; 2019.
3. C. Willman, A. Hakansson, O. Osifo, A. Backlin, and S.J. Svard, "Nondestructive Assay of Spent Nuclear Fuel with Gamma-ray Spectroscopy," *Annals of Nuclear Energy*, 33(5), pp. 427-438 (2006).
4. J. Cooper, "Radioanalytical Applications of gamma-gamma coincidence techniques with lithium drifted germanium detectors," *Analytical Chemistry* 1971 43(7), 838-845. doi: 10.1021/ac60302a017.
5. N. Svrkota, J. Mijušković, and N. M. Antović, "The Registration of Cs-134 by Gamma Detector Pairs at an Angle of  $90^\circ$ ," *Radiation and Applications*, 3(1), pp. 18-22 (2018), [www.rad-journal.org/paper.php?id=96#](http://www.rad-journal.org/paper.php?id=96#).
6. A.A. Sonzogni, "Decay Radiation Results," 2004, [www.nndc.bnl.gov/nudat2/decaysearchdirect.jsp?nuc=<sup>134</sup>CS&unc=nds](http://www.nndc.bnl.gov/nudat2/decaysearchdirect.jsp?nuc=<sup>134</sup>CS&unc=nds).
7. A. Drescher, M. Yoho, S. Landsberger, M. Durbin, S. Biegalski, D. Meier, and J. Schwantes, "Gamma-gamma coincidence performance of LaBr<sub>3</sub>:Ce scintillation detectors vs HPGe detectors in high count-rate scenarios," *Applied Radiation and Isotopes*, 122, pp. 116-210 (2017). doi:10.1016/J.APRADISO.2017.01.012.
8. J. Joshi, A. Trahan, and W. Charlton. "Absolute Measurement of  $^{137}\text{Cs}$  and  $^{134}\text{Cs}/^{137}\text{Cs}$  and  $^{154}\text{Eu}/^{137}\text{Cs}$  Ratios to Verify University of Texas TRIGA Reactor Spent Fuel BU," INMM Annual Meeting; Palm Desert, CA USA (2019).
9. Dynasil, "CLLBC Gamma-Neutron Scintillator," (2021) <https://www.dynasil.com/product-category/scintillators/cllbc-gamma-neutron-scintillator/>.
10. B. Löher, D. Savran, E. Fiori, M. Miklaveč, N. Pietralla, and M. Vencelj, "High count rate spectroscopy with LaBr<sub>3</sub>:Ce scintillation detectors," *Nucl. Instruments and Methods in Phys. Res. A*, 686, pp. 1–6 (2012). doi:10.1016/j.nima.2012.05.051.
11. XIA LLC, "XIA Pixie-16 User Manual," (2018). [https://xia.com/wp-content/uploads/2018/12/Pixie16\\_UserManual.pdf](https://xia.com/wp-content/uploads/2018/12/Pixie16_UserManual.pdf)